

Direct Observation of a Hydroperoxide Surface Intermediate upon Visible Light-Driven Water Oxidation at an Ir Oxide Nanocluster Catalyst by Rapid-Scan FT-IR Spectroscopy

Narayanappa Sivasankar,[†] Walter W. Weare,[‡] and Heinz Frei^{*}

Physical Biosciences Division, Lawrence Berkeley National Laboratory, University of California, Berkeley, California 94720, United States

S Supporting Information

ABSTRACT: A surface hydroperoxide intermediate has been detected upon oxidation of water at an Ir oxide nanocluster catalyst system under pulsed excitation of a $[\text{Ru}(\text{bpy})_3]^{2+}$ visible light sensitizer by recording of the OO vibrational mode at 830 cm^{-1} . Rapid-scan FT-IR spectroscopy of colloidal H_2O , D_2O , and D_2^{18}O solutions in the attenuated total reflection mode allowed spectral assignment of IrOOH on the basis of an observed D shift of 30 cm^{-1} , and ^{18}O shifts of 24 cm^{-1} ($^{16}\text{O}^{18}\text{O}$) and 46 cm^{-1} ($^{18}\text{O}^{18}\text{O}$). The laser pulse response of the infrared band is consistent with the kinetic relevancy of the intermediate. This is the first observation of a surface intermediate of oxygen evolution at an Ir oxide multielectron catalyst.

Recent progress in efficient water oxidation at Co or Mn oxide nanoclusters embedded in mesoporous silica^{1,2} or Co oxide electrodeposits³ has substantially expanded the range of abundant metal oxides that may be viable as oxygen-evolving catalysts for artificial photosynthesis. Metal oxide nanoclusters are attractive water oxidation catalysts because oxidizing charge injected into the catalyst particle is instantly stabilized in the form of a chemical change at any of the abundant catalytic surface sites, which is essential for maintaining high quantum efficiency at high solar intensity. Catalyst materials with the highest reported turnover rates per surface metal site are those of Ir and Ru, with IrO_2 as the chemically more stable oxide of the two under use.^{4,5} Recent detailed catalytic studies of nanoscale Ir oxide particles driven electrochemically^{6–9} or by a visible light sensitizer allowed the determination of the turnover frequency of surface Ir centers (between 6 and $10\text{ s}^{-1}\text{ Ir}_{\text{surf}}^{-1}$) and provided insights into the charge-transfer coupling between light absorber and catalyst.^{10–13} Interestingly, oxygen evolution has even been observed upon direct absorption of light by Ir oxide nanoclusters, although in this case the efficiency is much lower compared to that of hole transfer from a separate sensitizer or electrode in terms of both quantum yield and high overpotential of the holes generated.¹⁴

Elucidation of the step-by-step mechanism of the conversion of H_2O to O_2 on a noble metal oxide surface may provide valuable insights for oxygen-evolving solid oxide catalysts in general. Structure-specific in situ spectroscopy techniques like FT-IR are required to resolve elementary reaction steps, assess

kinetic barriers, and identify transient surface intermediates under photochemical reaction conditions. However, such measurements have not been reported to date for heterogeneous multielectron catalysts for water oxidation that can be driven by visible light. Here, we report the direct IR observation of a surface hydroperoxide intermediate upon water oxidation at IrO_2 nanoclusters in aqueous solution. The kinetic relevancy of the intermediate was confirmed by the laser pulse response of the transient IR signal of the visible light-sensitized catalyst.

A few in situ spectroscopic observations of water oxidation at metal oxide photo- or electrocatalysts have been reported recently. TiOOH and TiOOTi species were detected by IR spectroscopy upon UV irradiation of TiO_2 particulate films exposed to aqueous solution, although their kinetic relevancy could not be assessed under the steady-state photolysis conditions used.¹⁵ In the case of Co-containing electrocatalytic films deposited from phosphate-buffered Co^{II} solution, Co^{IV} species were observed by EPR spectroscopy ex situ after electrochemical water oxidation.¹⁶ In recent time-resolved optical studies, detection of transient holes upon oxidation of water at UV-photoexcited TiO_2 ¹⁷ and Fe_2O_3 particles¹⁸ has provided first insights into the hole dynamics of the water oxidation cycle in these photocatalytic materials. Evidence shows that four photons and therefore four holes are required for the production of one oxygen molecule.¹⁷ In terms of water oxidation at a metal anode, a surface hydroperoxide species has recently been reported upon steady-state electro-oxidation of water at a gold electrode.¹⁹

Rapid-scan FT-IR spectroscopy offers a sensitive method for monitoring vibrational absorptions of chemical species on the millisecond and longer time scale over a broad spectral range and is most suitable in the search for transient surface intermediates. Use of the attenuated total reflection (ATR) technique minimizes absorption by the intense IR H_2O bands of aqueous suspensions because the evanescent IR probe beam penetrates only a few micrometers into the solution.²⁰ We have employed an ATR accessory featuring a 3 mm diameter diamond plate with three reflections. An aqueous solution of Ir oxide catalyst particles was held atop the ATR plate in a homemade Teflon liquid cell (Figure S1).²¹ The pulsed 476 nm photolysis laser beam for excitation of the $[\text{Ru}(\text{bpy})_3]^{2+}$ sensitizer entered the liquid cell perpendicular to the ATR plate and passed through the aqueous solution in the direction of the diamond element. Synthesis and characterization of Ir oxide colloid (6 nm particles)

Received: June 8, 2011

Published: July 19, 2011

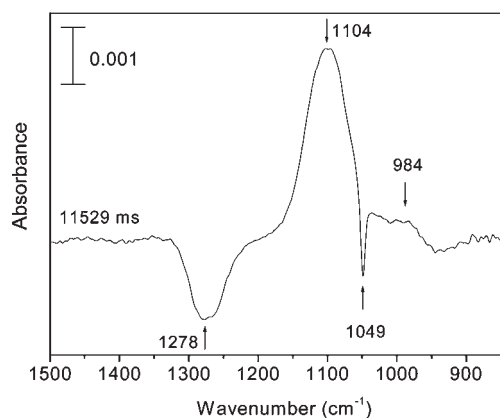


Figure 1. Rapid-scan FT-IR difference spectrum recorded 12 s after excitation of $[\text{Ru}(\text{bpy})_3]^{2+}$ sensitizer with a 1 s pulse at 476 nm (300 mW). The 1278 and 1049 cm^{-1} bands are due to $\text{S}_2\text{O}_8^{2-}$ depletion, and the peaks at 1104 and 984 cm^{-1} to growth of SO_4^{2-} .

in H_2O or D_2O was conducted according to the literature procedure.^{21,22} In a typical experiment, 1 mL of an aqueous solution of IrO_2 colloid with added silicate and bicarbonate buffer was introduced into the Teflon cell, followed by addition of 0.5 mL of an aqueous solution containing the sensitizer ruthenium tris-bipyridyl dichloride ($[\text{Ru}(\text{bpy})_3\text{Cl}_2]^{2+}$, 3 mg), persulfate acceptor ($\text{Na}_2\text{S}_2\text{O}_8$ (8 mg) + Na_2SO_4 (20 mg)), and buffer (NaSiF_6 (30 mg) + NaHCO_3). The final solution had a pH of 5.7. Details of the sample preparation, rapid-scan FT-IR measurement protocol, synchronization of the laser photolysis pulse, and data analysis are described in the Supporting Information.²¹

The FT-IR spectral trace of IrO_2 colloidal solution recorded 12 s after excitation of the $[\text{Ru}(\text{bpy})_3]^{2+}$ sensitizer with a 1 s pulse at 476 nm (300 mW) shows depletion of $\text{S}_2\text{O}_8^{2-}$ at 1278 and 1049 cm^{-1} with concurrent growth of SO_4^{2-} at 1104 and 984 cm^{-1} (Figure 1). The bands of these species are in good agreement with literature reports.^{23,24} No spectral changes are observed in the absence of light excitation, when applying a laser pulse with no $[\text{Ru}(\text{bpy})_3]^{2+}$ present, or in the absence of $\text{S}_2\text{O}_8^{2-}$. These observations confirm that transient oxidized $[\text{Ru}(\text{bpy})_3]^{3+}$ is generated by electron transfer from excited $[\text{Ru}(\text{bpy})_3]^{2+}$ to the persulfate acceptor (Scheme S1). Because transient sulfate radical anion ($\text{SO}_4^{\bullet-}$) formed upon one-electron reduction of $\text{S}_2\text{O}_8^{2-}$ is a strong oxidant ($\epsilon^0 = 2.4$ V (NHE)),²⁵ it spontaneously oxidizes another $[\text{Ru}(\text{bpy})_3]^{2+}$ in the dark, thereby generating a second $[\text{Ru}(\text{bpy})_3]^{3+}$ species for every persulfate species reduced.²⁶ Recording of the depletion of $[\text{Ru}(\text{bpy})_3]^{2+}$ by a 476 nm laser pulse in the presence of persulfate by time-resolved nanosecond optical absorption spectroscopy in our laboratory confirmed literature reports according to which spontaneous oxidation of $[\text{Ru}(\text{bpy})_3]^{2+}$ by $\text{SO}_4^{\bullet-}$ species is complete within 30 μs at the concentrations used (Figure S2).^{21,27} Similarly, our transient optical measurements agree with previous reports that electron transfer from IrO_2 catalyst to $[\text{Ru}(\text{bpy})_3]^{3+}$ proceeds in the 50–200 μs range for electrostatically adsorbed sensitizer molecules and within a few milliseconds for freely diffusing $[\text{Ru}(\text{bpy})_3]^{3+}$.²⁸ Therefore, oxidized sensitizer $[\text{Ru}(\text{bpy})_3]^{3+}$ molecules are present only when the visible laser pulse is on. During that period, electrons are pulled from the IrO_2 catalyst particles, resulting in evolution of O_2 , but water oxidation catalysis ceases as soon as the light pulse is off.

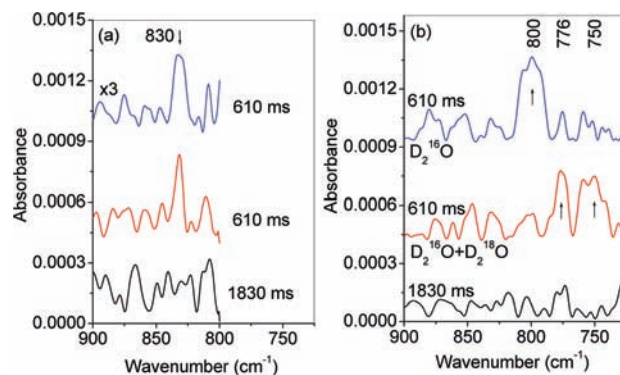


Figure 2. Rapid-scan FT-IR traces in the 900–700 cm^{-1} region. (a) 610 ms (light on) and 1830 ms spectra (light off) for the photo-oxidation of H_2O . The 610 ms slices from two separate experiments are shown to indicate the degree of uncertainty regarding band shape. The spectral region below 800 cm^{-1} exhibits high noise due to H_2O tumbling-mode absorption. (b) 610 ms slices of experiments in D_2^{16}O (top, average of 140 runs) and D_2^{16}O (33%) + D_2^{18}O (66%) (middle, average of 68 runs), along with the 1830 ms slice of the D_2^{16}O experiment (bottom).

Moreover, because of the many orders of magnitude higher concentration of $[\text{Ru}(\text{bpy})_3]^{2+}$ (2.7×10^{-3} M) compared to that of IrO_2 colloidal particles (2.3×10^{-7} M), transient sulfate radical anions oxidize exclusively sensitizer molecules, while $[\text{Ru}(\text{bpy})_3]^{3+}$ species drive the IrO_2 catalyst.

Using an IrO_2 colloidal solution identical to the one employed in the rapid-scan FT-IR experiment, electrochemical measurement of O_2 product buildup upon illumination with a 476 nm laser pulse of 1 s duration showed growth of oxygen within a few seconds (Figure S3).²¹ The asymptotic O_2 buildup was linear, with laser power in the 200–500 mW range, reaching 47 μmol of O_2 L^{-1} aqueous solution for a 225 mW laser pulse. The corresponding amount of surface intermediate is adequate for the detection of an IR band of moderate intensity by our ATR setup.

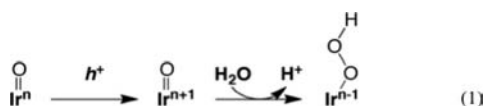
Comparison of consecutive rapid-scan FT-IR time slices following illumination of the colloidal solution by a 476 nm laser pulse of 1 s duration revealed an absorption band at 830 cm^{-1} which appeared only in the first (610 ms) spectrum but vanished completely in the following 1830 ms trace and all subsequent spectra (Figure 2a). The times indicated represent the midpoints of consecutive 1220 ms interferogram data acquisition periods, with the first (610 ms) overlapping with the photolysis pulse (light on) and the second (1830 ms) recording data after termination of the pulse (light off) ($t = 0$ is onset of photolysis pulse; details of the timing protocol are described in the Supporting Information, Scheme S2).²¹ The band position of 830 cm^{-1} is characteristic of an O–O single bond stretch of a peroxide moiety.²⁹ In order to maximize the detection sensitivity in this spectral region, D_2O was favored over H_2O as solvent because of the higher transmission of D_2O in the 800–700 cm^{-1} region compared to that of H_2O (Figure S4).²¹ The D isotope effect shifts the tumbling motion of the water molecule by tens of cm^{-1} to the red, resulting in higher transparency in the 900–730 cm^{-1} region for D_2O .³⁰ As in the case of the rapid-scan experiment with H_2O , bands of the 610 ms time slice of this spectral region in D_2O and partially ^{18}O -labeled D_2O were not present in the 1830 ms and subsequent traces. Figure 2b shows an absorption at 800 cm^{-1} for D_2^{16}O , while a D_2^{16}O (33%) + D_2^{18}O (66%) mixture exhibits peaks at 776 and 750 cm^{-1} , in

addition to a very weak band at 800 cm^{-1} . Peak shifts expected for an O–O stretch from the harmonic model are 23 cm^{-1} ($^{18}\text{O}^{16}\text{O}$) and 46 cm^{-1} ($^{18}\text{O}^{18}\text{O}$), in agreement with the observed isotopic shifts of 24 and 50 cm^{-1} , respectively. While the doubly labeled $^{18}\text{O}^{18}\text{O}$ absorption is observed, the shape and intensity of this band are considerably less certain than for the 776 cm^{-1} peak because of the steep decrease of transmission of the IR probe light around 750 cm^{-1} . The observed D isotope shift of 30 cm^{-1} indicates coupling of an OH (OD) bending mode with the OO stretch, thereby allowing us to identify the surface intermediate as a hydroperoxide (IrOOH) species.

Assignment to hydrogen peroxide can be ruled out because H_2O_2 absorbs at substantially higher frequency (877 cm^{-1}).³¹ Transition metal hydroperoxide groups such as TiOOH are known to absorb around 830 cm^{-1} .^{15,32} D isotope substitution of the hydroperoxide exhibits the expected red shift to lower frequency. The magnitude of the shift depends on the degree to which modes other than the OO stretch contribute to the normal mode, which may explain the larger shift of 80 cm^{-1} for another metal-hydroperoxide group, TiOOD ,³³ compared to the 30 cm^{-1} shift observed for IrOOD .

The turnover frequency of colloidal IrO_2 particles is $6\text{--}10\text{ O}_2$ molecules s^{-1} per Ir surface site according to electrochemical measurements,^{6–9} which implies a turnover time of 160 ms or faster. The fact that there is no IR band of the hydroperoxide observed in the spectral time slice following completion of the photolysis pulse indicates that the intermediate has an upper lifetime limit of a few hundred milliseconds. Therefore, the on/off laser pulse response of the IR band is consistent with IrOOH as a kinetically relevant intermediate of catalytic water oxidation. This is the first observation of a surface intermediate of oxygen evolution at an Ir oxide multielectron catalyst.

On the basis of this result, a partial mechanism for water oxidation at the Ir oxide nanoparticle surface, shown in eq 1, is proposed.



Most likely, the initial hole transferred from transient $[\text{Ru}(\text{bpy})_3]^{3+}$ to the IrO_2 cluster oxidizes an $\text{Ir}^{\text{IV}}=\text{O}$ surface site to $\text{Ir}^{\text{V}}=\text{O}$. The oxo oxygen so produced should be sufficiently electrophilic to react with a water molecule to form an OO bond, resulting in the observed $\text{Ir}^{\text{III}}\text{OOH}$ surface species. The two subsequent charge injection steps result in oxidation of $\text{Ir}^{\text{III}}\text{OOH}$ under elimination of O_2 . Hydration of the reduced Ir^{III} center so produced and reoxidation to $\text{Ir}^{\text{IV}}=\text{O}$ closes the catalytic cycle. This mechanism is consistent with the result of a combined pulse radiolysis–electrochemical study of IrO_2 colloid by Nahor et al. which suggests that Ir atoms in the +5 state are involved in the water oxidation cycle.³⁴ In light of electrochemical potential considerations of IrO_2 nanoparticle films,⁷ $\text{Ir}=\text{O}$ sites in oxidation state +6 ($n = +5$ in eq 1) undergoing electrophilic attack on water cannot be ruled out. The formation of doubly labeled $\text{Ir}^{18}\text{O}^{18}\text{OD}$ species when using Ir^{16}O_2 catalyst particles suspended in D_2^{18}O -containing solution is indicative of isotopic O exchange between Ir oxide particles and water molecules, in agreement with previous findings.³⁵ The mechanistic steps of eq 1 are similar to the water oxidation pathways proposed for mononuclear Ir³⁶ and Ru complexes.³⁷ Furthermore, a surface hydroperoxide intermediate in water oxidation at noble metal

oxides, including IrO_2 (110 face), is predicted by quantum thermochemical calculations.³⁸ Our observation of a surface hydroperoxide intermediate renders earlier proposals unlikely, such as direct $\text{O}=\text{O}$ formation between adjacent surface $\text{Ir}=\text{O}$ moieties as a major pathway, although sequential O–O single-bond formation of neighboring $\text{Ir}=\text{O}$ sites followed by hydrolysis to IrOOH cannot be ruled out.³⁵

In conclusion, a surface hydroperoxide species on a metal oxide multi-electron-transfer catalyst has been identified as an intermediate of water oxidation for the first time. The laser pulse response of the observed IR band is consistent with kinetic relevancy of the intermediate. On the basis of direct IR detection of the surface hydroperoxide, we propose a mechanism that results in O–O bond formation by the reaction of an Ir^{V} oxo intermediate with water or a hydroxide group. Experiments are in progress with submillisecond laser photolysis pulses, with the goal of resolving the kinetics of the surface hydroperoxide and detecting shorter-lived intermediates of the catalytic cycle.

■ ASSOCIATED CONTENT

S Supporting Information. Synthetic methods, rapid-scan ATR FT-IR instrumentation and measurement procedure, electrochemical O_2 measurement, and transient optical measurement. This material is available free of charge via the Internet at <http://pubs.acs.org>.

■ AUTHOR INFORMATION

Corresponding Author

HMFrei@lbl.gov

Present Addresses

[†]Liquid Light Inc., 7 Deer Park Dr., Suite F, Monmouth Junction, NJ 08852, United States.

[‡]Department of Chemistry, North Carolina State University, Raleigh, NC 27695, United States.

■ ACKNOWLEDGMENT

This work was supported by the Director, Office of Science, Office of Basic Energy Sciences, Division of Chemical, Geological and Biosciences of the U.S. Department of Energy under Contract No. DE-AC02-05CH11231. The authors thank Andreas Bachmeier for conducting the time-resolved optical measurements and Dr. Ryuhei Nakamura for preliminary experiments with the setup used in this work.

■ REFERENCES

- (1) Jiao, F.; Frei, H. *Angew. Chem., Int. Ed.* **2009**, *48*, 1841–1844.
- (2) Jiao, F.; Frei, H. *Chem. Commun.* **2010**, *46*, 2920–2922.
- (3) Kanan, M. W.; Nocera, D. G. *Science* **2008**, *321*, 1072–1075.
- (4) Trasatti, S. *Electrochim. Acta* **1984**, *29*, 1503–1512.
- (5) Harriman, A.; Pickering, I. J.; Thomas, J. M.; Christensen, P. A. *J. Chem. Soc., Faraday Trans. 1* **1988**, *84*, 2795–2806.
- (6) Nakagawa, T.; Bjorge, N. S.; Murray, R. W. *J. Am. Chem. Soc.* **2009**, *131*, 15578–15579.
- (7) Nakagawa, T.; Beasley, C. A.; Murray, R. W. *J. Phys. Chem. C* **2009**, *113*, 12958–12961.
- (8) Yagi, M.; Tomita, E.; Sakita, S.; Kuwabara, T.; Nagai, K. *J. Phys. Chem. B* **2005**, *109*, 21489–21491.
- (9) Kuwabara, T.; Tomita, E.; Sakita, S.; Hasegawa, D.; Sone, K.; Yagi, M. *J. Phys. Chem. C* **2008**, *112*, 3774–3779.

- (10) Morris, N. D.; Suzuki, M.; Mallouk, T. E. *J. Phys. Chem. A* **2004**, *108*, 9115–9119.
- (11) Youngblood, W. J.; Lee, S. H. A.; Kobayashi, Y.; Hernandez-Pagan, E. A.; Hoertz, P. G.; Moore, T. A.; Moore, A. L.; Gust, D.; Mallouk, T. E. *J. Am. Chem. Soc.* **2009**, *131*, 926–927.
- (12) Nakamura, R.; Frei, H. *J. Am. Chem. Soc.* **2006**, *128*, 10668–10669.
- (13) Han, H.; Frei, H. *J. Phys. Chem. C* **2008**, *112*, 16156–16159.
- (14) Frame, F. A.; Townsend, T. K.; Chamousis, R. L.; Sabio, E. M.; Dittrich, T.; Browning, N. D.; Osterloh, F. E. *J. Am. Chem. Soc.* **2011**, *133*, 7264–7267.
- (15) Nakamura, R.; Nakato, Y. *J. Am. Chem. Soc.* **2004**, *126*, 1290–1298.
- (16) McAlpin, J. G.; Surendranath, Y.; Dinca, M.; Stich, T. A.; Stoian, S. A.; Casey, W. H.; Nocera, D. G.; Britt, R. D. *J. Am. Chem. Soc.* **2011**, *132*, 6882–6883.
- (17) Tang, J.; Durrant, J. R.; Klug, D. R. *J. Am. Chem. Soc.* **2008**, *130*, 13885–13891.
- (18) Pendlebury, S. R.; Barroso, M.; Cowan, A. J.; Sivula, K.; Tang, J.; Graetzel, M.; Klug, D.; Durrant, J. R. *Chem. Commun.* **2011**, *47*, 716–718.
- (19) Yeo, B. S.; Klaus, S. L.; Ross, P. N.; Mathies, R. M.; Bell, A. T. *ChemPhysChem* **2010**, *11*, 1854–1857.
- (20) Harrick, N. J. *Internal Reflection Spectroscopy*; Wiley: New York, 1967.
- (21) See Supporting Information.
- (22) Hara, M.; Waraksa, C. C.; Lean, J. T.; Lewis, B. A.; Mallouk, T. E. *J. Phys. Chem. A* **2000**, *104*, 5275–5280.
- (23) Yang, C. Q.; Gu, X. *J. Appl. Polym. Sci.* **2001**, *81*, 223–228.
- (24) Baker, L. J.; Bowmaker, G. A.; Camp, D.; Healy, P. C.; Schmidbauer, H.; Steigelmann, O.; White, A. H. *Inorg. Chem.* **1992**, *31*, 3656–3662.
- (25) Stanbury, D. M. *Adv. Inorg. Chem.* **1989**, *33*, 69–72.
- (26) Bolletta, F.; Juris, A.; Maestri, M.; Sandrini, D. *Inorg. Chim. Acta* **1980**, *44*, L175–L181.
- (27) White, H. S.; Becker, W. G.; Bard, A. J. *J. Phys. Chem.* **1984**, *88*, 1840–1846.
- (28) Hoertz, P. G.; Kim, Y. I.; Youngblood, W. J.; Mallouk, T. E. *J. Phys. Chem. B* **2007**, *111*, 6845–6856.
- (29) Nakamoto, K. *Infrared and Raman Spectra of Inorganic and Coordination Compounds*, 5th ed.; Wiley: New York, 1997; p 155.
- (30) Socrates, G. *Infrared and Raman Characteristic Group Frequencies*, 3rd ed.; Wiley: New York, 2001; p 7.
- (31) Camy-Peyret, C.; Flaud, J. M.; Johns, J. W. C.; Noel, M. *J. Mol. Spectrosc.* **1992**, *55*, 84–91.
- (32) Lin, W.; Frei, H. *J. Am. Chem. Soc.* **2002**, *124*, 9292–9298.
- (33) Nakamura, R.; Imanishi, A.; Murakoshi, K.; Nakato, Y. *J. Am. Chem. Soc.* **2003**, *125*, 7443–7450.
- (34) Nahor, G. S.; Hapiot, P.; Neta, P.; Harriman, A. *J. Phys. Chem.* **1991**, *95*, 616–621.
- (35) Fierro, S.; Nagel, T.; Baltruschat, H.; Comminellis, C. *Electrochem. Commun.* **2007**, *9*, 1969–1974.
- (36) Hull, J. F.; Balcells, D.; Blakemore, J. D.; Incarvito, C. D.; Eisenstein, O.; Brudvig, G. W.; Crabtree, R. H. *J. Am. Chem. Soc.* **2009**, *131*, 8730–8731.
- (37) Concepcion, J. J.; Jurss, J. W.; Norris, M. R.; Chen, Z.; Templeton, J. L.; Meyer, T. J. *Inorg. Chem.* **2010**, *49*, 1277–1279.
- (38) Rossmeis, J.; Qu, Z. W.; Zhu, H.; Kroes, G. J.; Norskov, J. K. *J. Electroanal. Chem.* **2007**, *607*, 83–89.